Chemistry of Metals and Alloys

Chem. Met. Alloys 1 (2008) 137-139
Ivan Franko National University of Lviv
www.chemetal-journal.org

Phase equilibria in the $TiMn_2$–$TiFe_2$ polythermal section

V. IVANCHENKO[1]*, V. DEKHTYARENKO[1], T. KOSORUKOVA[1], T. PRYADKO[1]

[1] *Department of Phase Equilibria, G.V. Kurdyumov Institute for Metal Physics of NAS of Ukraine, acad. Vernadsky av. 36, 03142 Kyyiv, Ukraine*
* *Corresponding author. E-mail: ivanch@imp.kiev.ua*

Received September 19, 2007; accepted May 30, 2008; available on-line September 10, 2008

Fe-Mn-Ti alloys located along the line joining $TiMn_2$ and $TiFe_2$ and in the isopleth with 14 at.% Fe between 33.3 and 45 at.% Ti have been studied using DTA and X-ray diffraction. The polythermal section $TiMn_2$-$TiFe_2$ has been constructed. It is quasibinary with a cigar-type fusion diagram. The composition dependence of the crystallographic cell parameters obeys the Vegard rule. The existence of a sharp bend on the Ti-rich boundary of the $Ti(Mn,Fe)_2$ field at 14 at.% Ti was not confirmed.

$Ti(Mn,Fe)_2$ / Laves phases / Phase diagram

Introduction

The liquidus surfaces of the system Fe–Mn–Ti have been investigated by Murakami *et al.* [1] within a composition range from the Ti-corner of the compositional diagram to a line joining the compositions 0% Mn, 86 at.% Fe and 0% Fe, 83.5 at.% Mn. According to [1] the outstanding feature of the system within the investigated composition range is the formation of a complete series of solid solutions between the Laves phases $TiFe_2$ and $TiMn_2$. Discrepancies arise, however, within the primary $Ti(Mn,Fe)_2$ field. Although the contours reported in [1] are consistent with the liquidus temperature for the decomposition of $TiMn_2$ in the Mn–Ti system, the freezing point assumed for $TiFe_2$ by these workers appears to be much too high. The original diagram presented in [1] shows isotherms at 1500 °C penetrating in the ternary composition field, whereas according to [2] the melting point of $TiFe_2$ is much lower than 1500 °C. Raynor and Rivlin [3] accepted the melting point of $TiFe_2$ according to [2] as 1427 °C. For this reason the 1450 and 1500 °C isotherms were omitted by them, and the 1400 and 1450 °C isotherms were altered so that the temperatures conform the accepted binary Fe–Ti diagram from [4]. But these isothermal contours were not confirmed by experimental studies.

An important contribution to the study of the Fe-Mn-Ti phase diagram was made in the work by Dew-Hughes and Kaufman [5] by a direct experimental investigation of the system using electron-probe microanalysis (EPMA), mainly to establish the boundaries of the TiFe phase, but providing evidence with regard to the Ti-rich boundary of the $Ti(Mn,Fe)_2$ phase and the general nature of the equilibria. One of the most significant results of the EPMA studies consisted in the observation at 1000 °C of a new phase with the composition 54.9 at.% Ti and 35.9 at.% Mn, that could be derived from the binary Mn–Ti ρ-phase, or could be an entirely new phase. This result tends to confirm the existence of a ρ-phase in the binary Mn-Ti system. The EPMA results showed that the Ti-rich boundary of the $Ti(Mn,Fe)_2$ phase field bends sharply towards the Ti-corner when the Fe content falls to approximately 14 at.%.

This study has two aims. The first one consists in the more precise definition of the phase equilibria in the $TiMn_2$–$TiFe_2$ polythermal section. The second one consists in checking the abnormal solubility of Ti in the $Ti(Mn,Fe)_2$ phase at 14 at.% Fe reported by [5].

Sample preparation and experimental procedures

Ingots with a mass of 30 g were prepared by argon arc melting. The starting materials were titanium sponge TG-100 (HB = 96, 0.05 % Fe, 0.002 % Si, 0.005 % C, 0.009 % N, 0.034 % O), electrolytic manganese with a purity of 99.95 %, and carbonyl iron sintered in dry hydrogen with a purity of 99.97 %. The alloy compositions were located along the $TiMn_2$–$TiFe_2$ join and in the part of the isopleth with 14 at.% Fe between 33.3 and 45 at.% Ti.

The chemical compositions of the ingots were analyzed using fluorescent X-ray spectroscopy (VRA 30). Deviations of the alloy compositions from the nominal compositions were less than 0.25 at.%.

Table 1 Nominal composition of the alloys and DTA data.

#	at.% Fe	at.% Mn	at.% Ti	Temperature, °C	
				Solidus	Liquidus
1	0	66.7	balance	1325	1325
2	10	56.7	-"-	1335	1337
3	14	52.,7	-"-	1340	1350
4	20	46.7	-"-	1340	1355
5	30	36.7	-"-	1352	1365
6	40	26.7	-"-	1362	1392
7	50	16.7	-"-	1382	1415
8	14	46	-"-	1220	1327
9	14	41	-"-	1110	1310
10	66.7	0	-"-	1440	1440

Therefore the nominal compositions of the alloys are presented in Table 1. The alloys were annealed at 1000 °C (50 h). They were studied using DTA (VDTA 8M-3) and X-ray diffraction (DRON-3M) techniques. DTA was performed in Y_2O_3 crucibles at heating and cooling rates of 0.7 °C/s. The measurement accuracy was better than ±7 °C.

Experimental results and discussion

The DTA results are presented in Table 1. The corresponding fusion diagram is given in Fig. 1. It is of cigar type and resembles the diagram that can be constructed using the data of [1], but the liquidus temperatures are substantially lower than the values reported by [1]. The melting temperature of $TiFe_2$ was measured as 1440±7 °C. This value is 13 °C higher than the one accepted by [3,4], but 40 °C lower than the one reported by [6]. The melting temperature of $TiMn_2$ was measured as 1325±7 °C and coincides with the value accepted by [7].

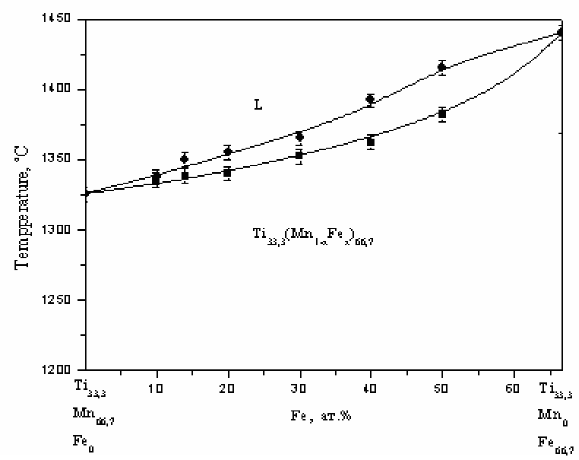

Fig. 1 Fusion diagram of the $TiFe_2$–$TiMn_2$ system.

The crystallographic cell parameters of $TiMn_2$ and $TiFe_2$ ($MgZn_2$ structure type) were measured as a = 483.0 pm, c = 792.3 pm, and a = 479.2 pm, c = 781.4 pm, respectively. The cell parameters as a function of the Fe content for the $TiMn_2$–$TiFe_2$ section obey the Vegard rule and may be presented as a = = 483.0 – $0.057X_{Fe}$ ± 0.3 pm, c = 792.3 – $0.163X_{Fe}$ ± ± 0.6 pm, where X_{Fe} is at.% Fe in the alloy.

The substitution of Mn for Ti in the Laves phase with 14 at.% Fe (alloys #3, #8, #9) leads to a decrease of the solidus and liquidus temperatures, as shown in Fig. 2. But the heating curve of $Ti_{45}Mn_{41}Fe_{14}$ (Fig. 3b) differs from the one of $Ti_{33.3}Mn_{52.7}Fe_{14}$ (Fig. 3a) by the presence of two additional calorific effects. The comparison of the heating and cooling curves presented in Fig. 3b with that of the binary alloy $Ti_{50}Mn_{50}$ (Fig. 4) [8], shows that they are very similar and differ only by the temperatures of the phase transformations. Hence, the additional calorific effects on the heating curve in Fig. 3b may be explained by the reactions (β-Ti) + $Ti_yFe_{14}Mn_z$ + ρ-TiMn ↔ L + ρ-TiMn (1110-1132 °C) and ρ-TiMn ↔ L + $Ti_yFe_{14}Mn_x$ (1132-1170 °C). Melting of the Laves phase is observed in the temperature interval 1170–1310 °C.

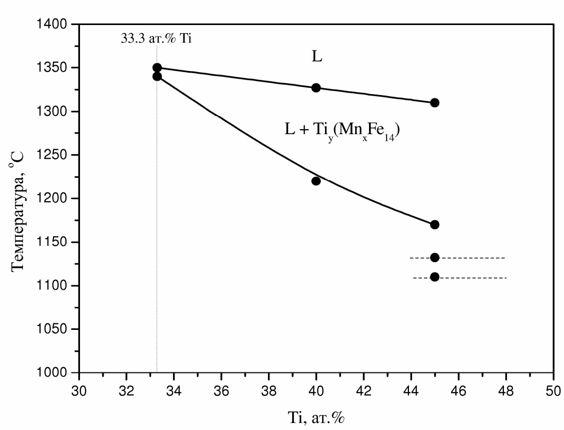

Fig. 2 The part of isopleth with 14 at.% Fe between 33.3 and 45 at.% Ti.

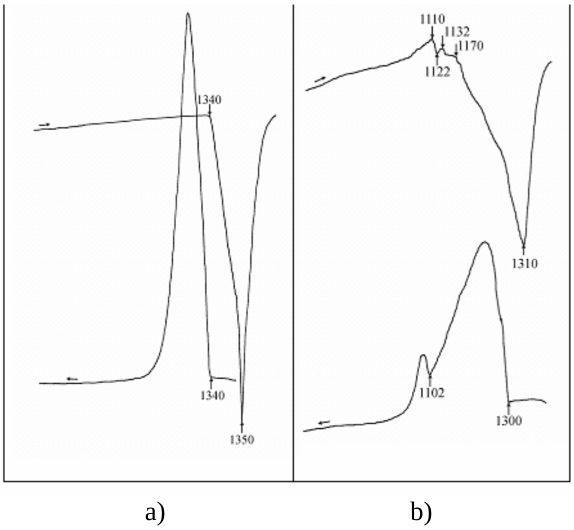

Fig. 3 Heating and cooling curves of the $Ti_{33.3}Mn_{52.7}Fe_{14}$ (a), and $Ti_{45}Mn_{41}Fe_{14}$ (b) alloys.

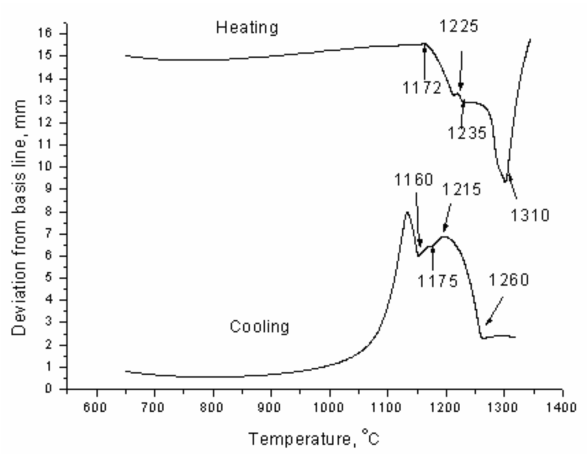

Fig. 4 Heating and cooling curves of the binary $Ti_{0.5}Mn_{0.5}$ alloy.

The existence of a ρ-phase in the $Ti_{45}Mn_{41}Fe_{14}$ alloy does not confirm the statement in [4] that the Ti-rich boundary of the $Ti(Mn,Fe)_2$ phase field bends sharply towards the Ti-corner when the Fe content falls to approximately 14 at.%.

For the part of the isopleth with 14 at.% Fe that is located between 33.3 and 45 at.% Ti the crystallographic cell parameters as a function of the Ti content may be presented as $a = 457.7 + 0.731\ X_{Ti} \pm 0.5$ pm, $c = 763.06 + 0.791\ X_{Ti} \pm 0.7$ pm, where X_{Ti} is at.% Ti in the alloy.

Conclusions

The polythermal section $TiMn_2$–$TiFe_2$ is quasibinary with a cigar-type fusion diagram. The melting points of $TiMn_2$ and $TiFe_2$ are 1325±7 and 1440±7 °C, respectively. The composition dependence of the cell parameters obeys the Vegard rule.

Since calorific effects caused by phase transformations with participation of a ρ-phase were observed in the $Ti_{45}Mn_{41}Fe_{14}$ alloy, the sharp bend of the Ti-rich boundary of the $Ti(Mn,Fe)_2$ field at 14 at.% Ti, reported earlier, is absent.

References

[1] Y. Murakami, Y. Yukawa, T. Enjyo, *Nippon Kinzoku Gakkaishi* 22 (1958) 265-269.
[2] A. Hellawell, W. Hume-Rothery, *Philos. Trans. R. Soc. London, Ser. A* 249 **(**1957) 417-454.
[3] G.V. Raynor, V.G. Rivlin, *Phase Equilibria in Iron Ternary Alloys*, Inst. Met., London, 1988, pp. 378-388.
[4] J.L. Murray, *Bull. Alloy Phase Diagrams* 2 (1981) 320-324.
[5] D. Dew-Hughes, L. Kaufman, *Calphad* 31 (1979) 175-203.
[6] I.I. Kornilov, N.G. Boriskina, *Dokl. Akad. Nauk SSSR* 108 (1956) 1083-1086 (in Russian).
[7] J.L. Murray, *Bull. Alloy Phase Diagrams* 2 (1981) 334-343.
[8] V.G. Ivanchenko, I.S. Gavrylenko, V.V. Pogorelaya, V.I. Nychyporenko, T.V. Pryadko, *Metaloznavstvo ta Obrobka Metaliv* (Metallurgy and Processing of Metals) 4 (2004) 16-20 (in Ukrainian).

Proceeding of the X International Conference on Crystal Chemistry of Intermetallic Compounds, Lviv, September 17-20, 2007.